




# STING is a prognostic factor related to tumor necrosis, sarcomatoid dedifferentiation, and distant metastasis in clear cell renal cell carcinoma

Stefano Marletta<sup>1,2</sup> · Anna Caliò<sup>1</sup> · Giuseppe Bogina<sup>3</sup> · Mimma Rizzo<sup>4</sup> · Matteo Brunelli<sup>1</sup> · Serena Pedroni<sup>1</sup> · Lisa Marcolini<sup>2</sup> · Lavinia Stefanizzi<sup>2</sup> · Stefano Gobbo<sup>5</sup> · Alessandro Princiotta<sup>6</sup> · Camillo Porta<sup>7</sup> · Angela Pecoraro<sup>8,9</sup> · Alessandro Antonelli<sup>6</sup> · Guido Martignoni<sup>1,2</sup> 

Received: 4 December 2022 / Revised: 21 February 2023 / Accepted: 21 April 2023 / Published online: 29 April 2023  
© The Author(s) 2023

## Abstract

STING is a molecule involved in immune reactions against double-stranded DNA fragments, released in infective and neoplastic diseases, whose role in the interactions between immune and neoplastic cells in clear cell renal cell carcinoma has not been studied yet. We investigated the immunohistochemical expression of STING in a series of 146 clear-cell renal cell carcinomas and correlated it with the main pathological prognostic factors. Furthermore, tumoral inflammatory infiltrate was evaluated and studied for the subpopulations of lymphocytes. Expression of STING was observed in 36% (53/146) of the samples, more frequently in high-grade (G3–G4) tumors (48%, 43/90) and recurrent/metastatic ones (75%, 24/32) than in low grade (G1–G2) and indolent neoplasms (16%, 9/55). STING staining correlated with parameters of aggressive behavior, including coagulative granular necrosis ( $p = 0.001$ ), stage ( $p < 0.001$ ), and development of metastases ( $p < 0.001$ ). Among prognostic parameters, STING immune expression reached an independent statistical significance ( $p = 0.029$ ) in multivariable analysis, along with the stage and the presence of coagulative granular necrosis. About tumor immune-environment, no significant statistical association has been demonstrated between tumor-infiltrating lymphocytes and STING. Our results provide novel insights regarding the role of STING in aggressive clear cell renal cell carcinomas, suggesting its adoption as a prognostic marker and a potentially targetable molecule for specific immunotherapies.

**Keywords** Clear cell renal cell carcinomas · STING · Immunohistochemistry · Cancer immune infiltrate · Tumor-infiltrating lymphocytes · Prognosis

---

Stefano Marletta and Anna Caliò contributed equally to this work.

✉ Guido Martignoni  
guido.martignoni@univr.it

<sup>1</sup> Department of Diagnostic and Public Health, Section of Pathology, University of Verona, Largo L. Scuro 10, 37134 Verona, Italy

<sup>2</sup> Department of Pathology, Pederzoli Hospital, Peschiera del Garda, Italy

<sup>3</sup> Department of Pathology, IRCCS Sacro Cuore Don Calabria Hospital, Negrar, Italy

<sup>4</sup> Division of Medical Oncology, A.O.U. Consorziiale Policlinico di Bari, Bari, Italy

<sup>5</sup> Department of Translational Medicine, University of Ferrara, Ferrara, Italy

<sup>6</sup> Department of Urology, University of Verona, Verona, Italy

<sup>7</sup> Interdisciplinary Department of Medicine, University of Bari “A. Moro”, Bari, Italy

<sup>8</sup> Department of Urology, San Luigi Gonzaga Hospital, University of Turin, Orbassano, Turin, Italy

<sup>9</sup> Department of Urology, Pederzoli Hospital, Peschiera del Garda, Italy

## Introduction

Stimulator of interferon genes (STING), also known as transmembrane protein 173 (TMEM173), is a molecule physiologically placed on the endoplasmic reticulum which regulates several aspects of the immune response to intracellular double-stranded DNA fragments [1]. Namely, these latter ones prompt the enzyme cyclic GMP-AMP synthase (cGAS) to produce cyclic GMP-AMP which then binds two molecules of STING [2]. This causes STING to translocate to the Golgi network and, through interactions with transcriptional factors such as interferon regulatory factor 3 (IRF3) and nuclear factor kappa B (NF $\kappa$ b), to activate the transcription of key inflammatory genes, including IL-6, tumor necrosis factor (TNF), and interferon (IFN)  $\alpha$  and  $\beta$  [3]. In humans, STING is mainly expressed by different types of immune cells, like T lymphocytes, macrophages, dendritic cells, and plasmacytoid dendritic cells, which activate its signaling pathway in response to double-stranded DNA molecules deriving from either exogenous or endogenous sources [4]. Thus, this not only explains why is STING involved in physiological inflammatory reactions against bacterial [5] and viral agents [6, 7] but also why it plays a significant role in regulating the complex immune response occurring in both autoimmune diseases, such as systemic lupus erythematosus [8] and rheumatoid arthritis [9], and, ultimately, cancer. Specifically, several studies have suggested that *STING* may act as either an oncogene or a tumor suppressor gene in some of the most common human cancers, such as colon [10], lung [11], and breast [12] carcinomas. As far as renal tumors are concerned, strong immunohistochemical expression of STING has been recently described in perivascular epithelioid cell (PEC) lesions of the kidney, while MiT family translocation renal cell carcinomas have been shown to stain negative for this marker [13]. Regarding other renal cell carcinomas, high STING mRNA levels and high immunohistochemical cytoplasmic expression of STING have been reported in renal medullary renal cell carcinoma [14], supporting further studies assessing the role of the cGAS-STING pathway in the immunotherapy of this tumor. Although in the last years, the role of the immune system in the biology of clear cell renal cell carcinoma has been extensively studied, no data regarding the cGAS-STING pathway are available. Therefore, in this study, we investigated STING immunohistochemical expression and its potential diagnostic and biological implications in a series of clear cell renal cell carcinomas.

## Methods

### Pathological features

One hundred forty-six clear cell renal cell carcinomas were retrieved from the files of participating institutions,

including samples from both primary neoplasms and distant metastasis when available. Data were recorded from electronic health databases. All procedures performed in our study involving human participants received institutional review board approval and were in accordance with the ethical standards of the institutional and/or national research committee and with the declaration of Helsinki. All patients gave their written informed consent to diagnostic procedures and treatment according to institutional rules for everyday clinical practice and experimental evaluations on archival tissue. All slides were reviewed by three authors (S.M., A.C., G.M.). Regarding morphological features, each tumor was evaluated for the nucleolar grade according to the International Society of Urological Pathology (ISUP) and WHO 2022 classification, the state of surgical margins, the pTNM stage according to the 8th edition of the AJCC Cancer Staging Manual, the presence/absence of a sarcomatoid component, the percentage of coagulative-granular necrosis, and the presence/absence of tumor-infiltrating lymphocytes. As for the stage, tumors were gathered into three categories: stages I–II (low stage), stage III (intermediate stage), and stage IV (high stage). According to the distribution of tumor-infiltrating lymphocytes in or around the cancer cells, the inflammatory infiltrate was graded in three categories as suggested by previous studies [15, 16]: “desert” (tumor-infiltrating lymphocytes absent either within the tumor or its periphery), “excluded” (tumor-infiltrating lymphocytes accumulate around the tumor but without relevant infiltration within the lesion), and “inflamed” (tumor-infiltrating lymphocytes are intermixed with the neoplastic cells in the entire tumor area). Follow-up data on the development of distant metastases and/or local recurrence, defined as further tumor detection at the site of previously performed surgical procedures, were recorded from electronic health databases relying on the available radiological and pathological records.

### Immunohistochemistry

Sections from tissue blocks of all cases were immunohistochemically stained with STING (anti-TMEM173; clone SP338, dilution 1:150; Abcam, UK). Heat-induced antigen retrieval for STING was performed using a microwave oven and 0.01 mol/L of citrate buffer, pH 8.0, for 30 min. Moreover, tumors defined as “excluded” and “inflamed” by hematoxylin and eosin were investigated for the specific composition of different lymphocytes subpopulations, according to the different percentages of expression of the following antibodies: CD3 (clone PS1, dilution 1:200, LEICA), CD20 (clone L26, prediluted, NOVOCASTRA), CD4 (clone 4B12, dilution 1:150, LEICA), CD8 (clone

29S, dilution 1:20, LEICA), and FOXP3 (clone 221D/D3, dilution 1:200, SEROTEC). All samples were processed using a sensitive “Bond Polymer Refine” detection system in an automated bond immunohistochemistry instrument (Leica Biosystems, Germany). Sections incubated without the primary antibody served as a negative control. Cytoplasmic and membranous labeling for the STING was recorded by combining the percentage of positive cells (0–100%) multiplied by staining intensity (0, 1+, 2+, and 3+) to obtain an overall H-score (0–300).

## Statistical analysis

For statistical analysis, data were imported and performed using STATA/IC for Windows version 14.0. Differences in distribution and frequency between clinicopathologic characteristics, distribution of tumor-infiltrating lymphocytes, and STING expression were analyzed using the  $\chi^2$  test, distinguishing between low (H-score  $\leq 5$ ) and high (H-score  $> 5$ ) levels of STING. As for the ISUP/WHO nucleolar grade, while G1 and G2 were collected together, G3 and G4 were considered separately. In detail, as suggested by previous works [17], the statistical analysis was conducted both by gathering G3 neoplasms displaying foci of necrosis with G4 ones as well as distinguishing G3 and G4 tumors individually regardless of the presence of necrosis.

Time to recurrence was calculated from the date of surgery to the date of recurrence or metastasis. Patients alive and not relapsing were censored at the date of their last follow-up visit. The cumulative incidence of time to recurrence in the groups was described by the Kaplan–Meier method and compared with the use of the log-rank test. The Cox proportional hazard regression model was used to evaluate the associations between clinicopathological factors and clinical outcomes. A two-sided *p*-value  $< 0.05$  was considered statistically significant.

## Results

### Clinical features

Forty-one patients were females, and one hundred-three were males (F:M ratio 1:2.5). Age at diagnosis ranged from 32 to 91 years (mean 64, median 65). At the time of the diagnosis, according to the pTNM classification, 66 patients were considered as low stage (I–II), 65 as intermediate stage (III), and 12 as high stage (IV); no data was available for the remaining three of them. Follow-up was available for 139 patients, ranging from 1 to 149 months (mean 41, median 9). Thirty-two patients displayed aggressive clinical behavior developing local recurrence (3 cases) and/or distant metastases (29 cases) after 34 months on average (range

from 1 and 129 months, median 6) since the diagnosis of the primary renal tumor. The site of metastatic disease was variable involving abdominal lymph nodes (5 cases), the lungs (21 cases), the pancreas (8 cases), the adrenal glands (9 cases), the brain (4 cases), the liver (3 cases), the thyroid gland (1 case), the urinary bladder (1 case), the colon (1 case), the peritoneum (1 case), and the vagina (1 case). Microscopic involvement of surgical resection margins (R1) was only detected in 3 of the samples (cases 76, 78, and 84), none of them developing local recurrence nor distant metastases on follow-up. Regarding systemic therapies in metastatic patients, most of them were given tyrosine-kinase inhibitors (TKI), while in one case (patient 71), a combination between a TKI (axitinib) and an immune-checkpoint inhibitor (ICI) (pembrolizumab) was administered. One of the patients (case 31) simultaneously underwent pancreatic resection for a neuroendocrine tumor, while another one (case 15), during follow-up, was diagnosed with colon cancer and afterward treated for it. Moreover, following surgical treatment of renal cell carcinoma, one patient was diagnosed with both prostatic adenocarcinoma and diffuse large B cell lymphoma (case 119), whereas another suffered from infiltrating high-grade bladder urothelial carcinoma with skull metastases (case 89).

### Pathological and immunohistochemical findings

One hundred-one patients underwent radical nephrectomy, while in the other 43 cases, the neoplasms were removed by partial nephrectomy. In two specimens, two different clear cell renal carcinomas were found within the same kidney (cases 112 and 137). The tumors ranged in size from 1.2 to 17 cm (mean 6, median 5). As for the nucleolar grade, according to the ISUP/WHO 2022 system, 55 tumors were classified as low-grade (G1–G2) while 90 of them as high-grade neoplasms, namely, 56 G3 and 34 G4. In twelve samples, all belonging to the high-grade (G4) group, a variable amount of sarcomatoid dedifferentiation was observed, being of rhabdoid type in 4 of them. In one case, information regarding the nucleolar grade of the primary renal tumor was not available, as only slides from a pancreatic metastasis were retrieved (case 37). All but three patients who developed metastatic diseases were affected by high-grade primary tumors (G3–G4). Foci of coagulative granular necrosis were detected in 54 tumors, 98% of which (53/54) displayed high nucleolar grade (G3–G4). Tumor-associated inflammatory infiltrate was scored as desert in 72% (105/146) and as either “excluded” or “inflamed” in 28% (41/146) of the samples, the majority of these latter (80%, 33/41) belonging to the high grade (G3–G4) group: namely, all but three of the 25 “inflamed” cases (88%) were represented by morphologically aggressive tumors (G3–G4), while the 16 “excluded” samples with peripheral limited

tumor-infiltrating lymphocytes' accumulation were slightly more evenly distributed between low-grade (31%) and high-grade (69%) neoplasms.

Membranous/cytoplasmic immunohistochemical expression of STING, considered as an H-score  $> 5$  (spanning from 5 to 290), was found in 53 of 146 samples (36%), including 9 of the 55 low-grade (G1–G2) tumors (16%), and 43 of the 90 high grade (G3–G4) carcinomas (48%) (Fig. 1), and one pancreatic metastasis, which represented the only available specimen from the corresponding case (patient 37). As for high-grade (G3–G4) tumors, positive immunolabelling for STING (H-score  $> 5$ ) was noticed in 21 of the 56 G3 neoplasms (37%) and 22 of the 34 G4 ones (65%). In addition, 58% (7/12) of the tumors showing a sarcomatoid component stained positive for STING, with an overall H-score ranging from 10 to 290. Furthermore, 64% (34/53) of the tumors displaying variable foci of necrosis were labeled positive for STING (H-score spanning from 10 to 290). About clinically aggressive tumors, immunolabelling for STING was recorded in 24 of 32 neoplasms (75%), variably observed in primary tumors and metastatic lesions, with an H-score ranging from 10 to 250 (Fig. 2).

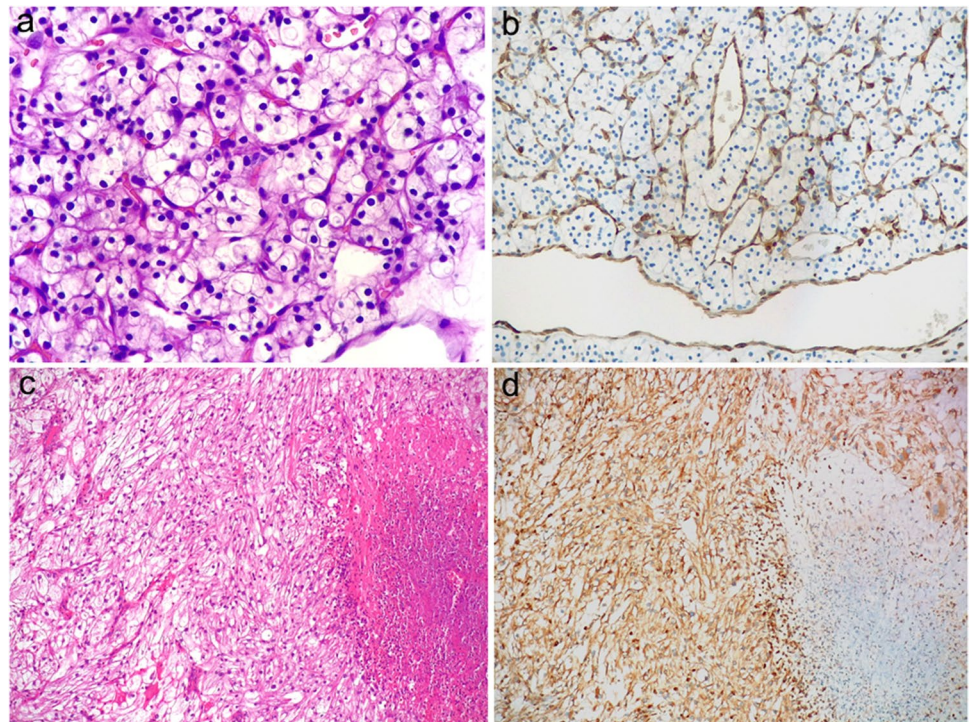
As for the specific composition of tumor-infiltrating lymphocytes, generally, both “excluded” and “inflamed” samples showed a prevalent  $CD3^+$  T-lymphocytes related response, variably making up from 50 to 95% of overall immune cells, while  $CD20^+$  B-lymphocytes accounted

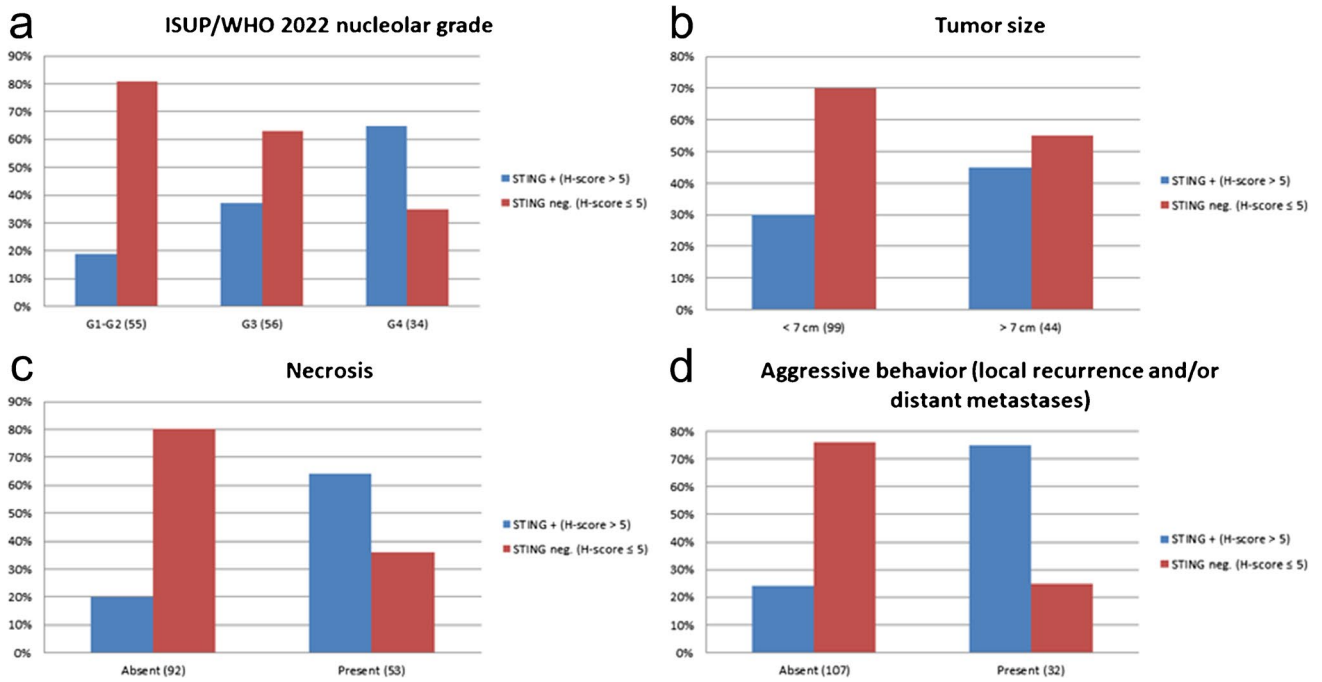
for a restricted proportion of all the inflammatory cells. Just a few scattered  $FOXP3^+$  T-regulatory lymphocytes were detected in each of the samples. In detail, a  $CD8^+$  T-cytotoxic response was significantly prevalent in those tumors effaced by a remarkable inflammatory infiltrate (Fig. 3). Conversely, “excluded” cases not only revealed a less prominent T-lymphocytes response than “inflamed” ones, with a mean higher amount of  $CD20^+$  B-lymphocytes, but they also showed a slightly more homogenous distribution of  $CD8^+$  T-cytotoxic lymphocytes and  $CD4^+$  T-helper lymphocytes.

In normal renal parenchyma, cytoplasmic STING expression was found in the cells of the vascular pole of glomeruli, likely the juxtaglomerular apparatus, in the endothelial cells of glomerular capillaries, and the interstitial stromal cells (Fig. 4). As for renal tubules, variable staining of STING was seen in the collecting ducts and the distal tubules, whereas the proximal tubules were constantly negative. Positive labeling for STING was found in endothelial cells and the smooth muscle cells of the vessels' wall within both normal parenchyma of the kidney and tumor lesions as well. Finally, a variable proportion of peritumoral and intratumoral lymphocytes in “excluded” and “inflamed” neoplasms, different from case to case, showed immune expression of STING.

Clinical, pathological, and immunohistochemical features of the present series are summarized in Table 1 and further specifically detailed in supplementary Table S1.

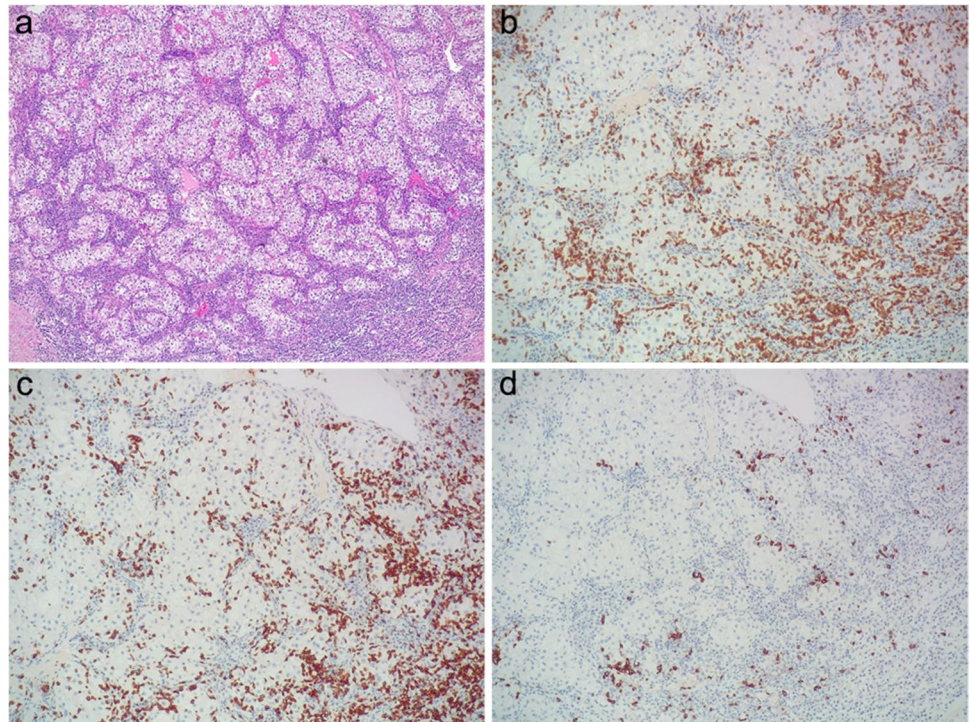
**Fig. 1** Low-grade clear cell renal cell carcinoma (a) staining negative for STING in neoplastic cells; conversely, endothelial cells of intratumoral capillaries labeled positive for STING (b). High-grade clear cell renal cell carcinoma (c) showing strong and diffuse immunohistochemical expression of STING, apart from a necrotic area on the left (d) (original magnification 100 $\times$  (c and d), 200 $\times$  (b) and 400 $\times$  (a))





**Fig. 2** Charts showing the correlation between STING immunohistochemical expression and ISUP/WHO 2022 grading, tumor size, presence of coagulative granular necrosis, and development of an aggressive clinical behavior

**Fig. 3** An example of “inflamed” clear cell renal cell carcinoma (a), showing a marked peritumoral and intratumoral infiltrate enriched with CD3<sup>+</sup> T lymphocytes (b), especially of the CD8<sup>+</sup> T-cytotoxic subset (c), and only a few CD20<sup>+</sup> B lymphocytes (d) (original magnification 50× (a), 100× (b, c, d))



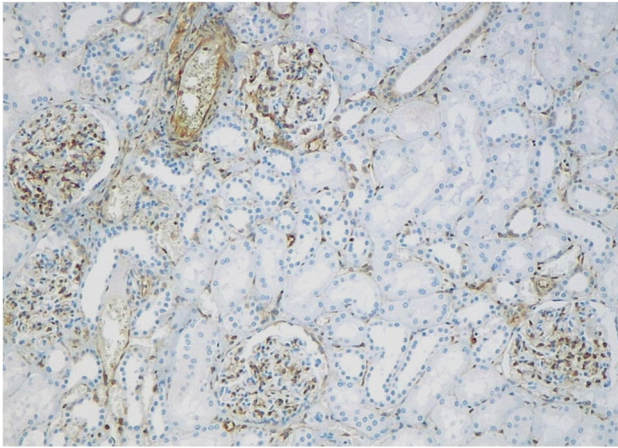


**Fig. 4** Normal renal parenchyma displaying variable staining for STING in the endothelial cells of the vascular pole of glomeruli and blood vessels, as well as in these latter ones' smooth muscle layer and in interstitial stromal cells (original magnification 100×)

### Statistical correlation between STING immunohistochemical expression, clinicopathological variables, and distribution of tumor-infiltrating lymphocytes

Using the chi-square test, a statistically relevant association was observed between STING positive immunohistochemical staining stratified according to the H-score and male sex ( $p = 0.024$ ), high pTNM stage ( $p < 0.001$ ), presence of necrosis ( $p = 0.001$ ), and high ISUP/WHO 2022 nucleolar grade, this latter both considering G3 tumors whether ( $p < 0.001$ ) or not ( $p < 0.001$ ) they showed foci of coagulative necrosis. As for inflammation, no association was found with STING expression, neither when considering “desert” plus “excluded” versus “inflamed” tumors ( $p = 0.073$ ) nor when matching “desert” versus “excluded” plus “inflamed” neoplasms ( $p = 0.669$ ).

Kaplan-Meier statistics demonstrated that STING expression was associated with a higher probability of disease recurrence/metastases ( $p < 0.001$ ), as well as high nucleolar grade ( $p = 0.0004$  and  $p < 0.001$ ), presence of

**Table 1** Summary of clinical-pathological features of renal cell carcinomas of the present series

Parameter	No. of cases (%)	Parameter	No. of cases (%)
Sex		Margin status	
F	41 (28)	R0	142 (98)
M	103 (72)	R1	3 (2)
Age	32–91 y.o., median 65	Necrosis	
Size		Absent	92 (63)
≤ 7 cm	99 (69)	Present ≤ 10%	33 (23)
> 7 cm	44 (31)	Present > 10%	20 (14)
Laterality		STING IHC	
Right	70 (48)	Negative	90 (62)
Left	75 (52)	Low (≤ 10%)	18 (12)
ISUP/WHO Grading		High (> 10%)	38 (26)
1	9 (6)	H-score	
2	46 (32)	≤ 5	93 (64)
3	56 (39)	> 5	53 (36)
4	34 (23)	Inflammatory infiltrate	
pTNM stage		Desert	105 (72)
I	59 (40)	Excluded	16 (11)
II	4 (3)	Inflamed	25 (17)
III	55 (38)	Follow up, months	1–149 (mean 41)
IV	28 (19)	Clinical behavior	
Surgery		NED	107 (77)
Radical nephrectomy	101 (70)	Local recurrence	3 (2)
Partial nephrectomy	43 (30)	Metastases	29 (21)

NED no evidence of disease

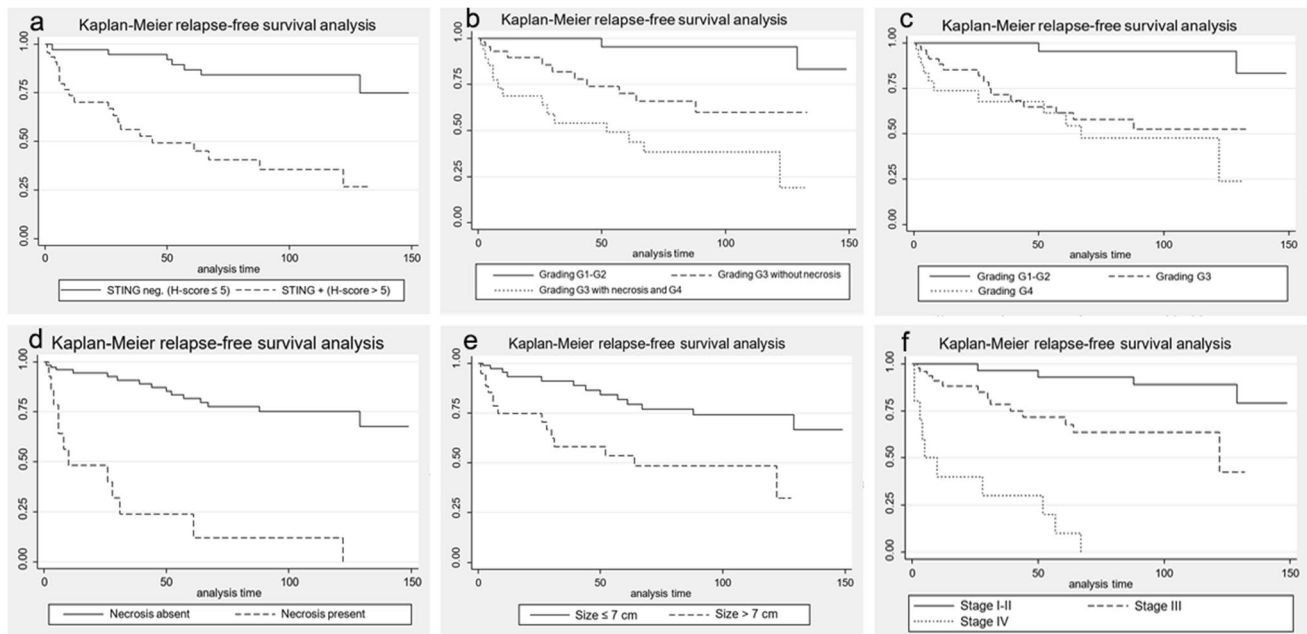


**Fig. 5** Kaplan-Meier curves analyzing the association between the development of recurrence or distant metastases and STING immunohistochemical expression (a), ISUP/WHO 2022 nucleolar grading (b, c), presence/absence of necrosis (d), tumor size (e), and pTNM tumor stage (f)

coagulative granular necrosis ( $p < 0.0001$ ), high pTNM stage ( $p < 0.001$ ), and large tumor size ( $p = 0.0007$ ) (Fig. 5). When a Cox proportional hazard regression model was employed for carrying a multivariable analysis among STING immunohistochemical expression, tumor size, nucleolar grade, coagulative granular necrosis, and clinical outcome, immunolabeling for such marker ( $p = 0.029$ ), presence of necrosis ( $p = 0.026$ ), and pTNM stage ( $p = 0.002$ ) reached a statistical independent significance (Table 2).

## Discussion

Despite the advances obtained regarding tumor biology and the development of more efficient therapeutic agents, clear cell renal carcinoma and, generally, kidney cancer still constitute a health problem of major concern in Western countries. In fact, during their lifetime, more than half of clear cell renal cell carcinoma patients develop synchronous or metachronous metastases and are then currently treated with combinations of ICIs and TKIs [18].

STING is a molecule involved in the inflammatory reaction to microbes, like viruses and bacteria, whose function has been recently shown to potentially modulate cancer immune response in several kinds of human malignancies. On these bases, in the present study, we have evaluated the immunohistochemical expression of STING in a broad series of clear cell renal cell carcinomas with different

clinical behavior. We have found an increased immunohistochemical expression of STING in 75% (24/32) of metastatic or locally aggressive clear cell renal cell carcinomas in contrast to clinically indolent ones (23%, 26 of 114 tumors). Not only STING immunohistochemical expression in our series was significantly correlated with the development of recurrence or distant metastasis ( $p < 0.001$ ), but it also reached a statistically independent meaning ( $p = 0.029$ ) in multivariable analysis, along with pTNM stage and the presence of coagulative granular necrosis. This finding suggests its employment as a further useful parameter of adverse clinical behavior, along with other ones already known for harboring prognostic value, including tumor size, ISUP/WHO nucleolar grading, and coagulative granular necrosis [19–22]. Interestingly, a wide amount (18 of 26 cases, 69%) of not-metastatic

**Table 2** Multivariable analysis concerning the main clinicopathological parameters and STING expression

Variable	HR (95% CI)	<i>p</i> value
Surgery	3.18 (0.38–26.45)	0.283
ISUP/WHO Grading	0.58 (0.24–1.37)	0.219
Necrosis	3.24 (1.14–9.15)	<b>0.026</b>
pTNM stage	5.50 (2.40–12.57)	<b>&lt; 0.001</b>
STING	3.37 (1.13–10.04)	<b>0.029</b>

HR hazard ratio, CI confidence interval

Statistically relevant results ( $p < 0.05$ ) are highlighted in bold

neoplasms positive for STING variably showed either high nucleolar grade (G3–G4), coagulative granular necrosis, or both. It is possible to hypothesize that these tumors are likely to harbor metastatic potential and then spread subsequently to other organs with a longer follow-up.

A possible explanation of STING expression in aggressive clear cell renal cell carcinomas may be its relationship with abnormal oxidative stress. It has been stated that a genomic signature characterized by overexpression of oxidative stress-related genes is significantly related to the probability of developing lymph nodes metastasis in clear cell renal cell carcinomas [23, 24]. Similarly, abnormal oxidative stress induces persistent DNA damage, alteration of function of proteins of the nuclear membrane and thus of its integrity [25], the release of blebs containing genomic damaged double-stranded DNA from the cytoplasm [26], and, ultimately, triggering of the cGAS-STING machine [2].

Since the cGAS-STING pathway has a role in immunoregulatory signaling, we have also evaluated the inflammatory infiltrate in our series and its correlation with STING immunohistochemical expression. Tumor-associated inflammatory infiltrate was observed in 28% of the tumors, most of them with high nucleolar grade (G3–G4). Interestingly, all but three of the 25 “inflamed” cases were represented by morphologically aggressive tumors and the tumor-associated inflammatory infiltrate was characterized by a CD8<sup>+</sup> T-cytotoxic response. Conversely, “excluded” tumors not only revealed a less prominent T-lymphocytes response than “inflamed” ones, with a mean higher amount of CD20<sup>+</sup> B-lymphocytes, but they also showed a slightly more homogenous distribution of CD8<sup>+</sup> T-cytotoxic lymphocytes and CD4<sup>+</sup> T-helper lymphocytes.

When analyzing the correlation between STING expression and tumor-associated infiltrate, no significant statistical association emerged from our study. In detail, immunohistochemical expression of STING did not correlate with tumor-infiltrating lymphocytes neither when matching “desert” plus “excluded” versus “inflamed” tumors ( $p = 0.073$ ) nor when performing statistical analysis of “desert” neoplasms versus “excluded” plus “inflamed” ones ( $p = 0.669$ ). A possible explanation of this finding may be linked to a different result of the activation of the cGAS-STING pathway in biologically aggressive neoplasms [1]. While low activation levels of this pathway seem to sustain a T-cytotoxic antitumoral effect via a type I interferons-mediated response [27, 28], chronic persistence of DNA damage and release of double-stranded DNA particles with subsequent c-GAS-STING activation may be responsible for a down-regulation of a cancer-related immune response. This likely occurs through the production of immunosuppressive cytokines and the induction of a senescence-associated secretory phenotype [29, 30], which ultimately leads to

the proliferation of tumor cells and the development of metastasis [12, 31]. Namely, recent elegant studies on triple-negative breast cancer lines and animal models have shown that chromosomal instability in neoplastic cells may trigger the cGAS-STING pathway via the formation of micronuclear vesicles [32]. Through a non-canonical NF- $\kappa$ B activation, this could cause IL6 expression to increase and then to up-regulate the STAT3-dependent signaling, ultimately leading to cancer cell survival and silencing of tumor-related inflammatory response. Such findings contribute to explaining why the loss of function of genes of the *cGAS-STING* pathway is only rarely encountered in chromosomally unstable cancers. Similarly, it has been recently reported that high IL6 levels are associated with poorer outcomes and lower treatment response in renal cell carcinoma patients [33]. Thus, the absence of a correlation between STING immunohistochemical expression and the increasing amount of CD8<sup>+</sup> T-cytotoxic lymphocytes intratumoral inflammatory infiltrate in our series may further strengthen the hypothesis of an immune-suppressive role for this pathway in morphologically aggressive renal cell carcinomas. The reduced anti-tumoral immune response in these settings of tumors, related to the activation of the STING pathway, may help these neoplasms to fully gain a metastatic potential.

From a therapeutic point of view, it has been demonstrated that patients with higher levels of tumor-infiltrating lymphocytes are more likely to respond to immune checkpoint modulators [34], which are nowadays a milestone for advanced renal cancer treatment [35–37]. Blockage of the STING pathway in morphologically aggressive renal cell carcinomas prevents local progression and metastasis development, eliciting a stronger antitumoral response [38]. Accordingly, in the aforementioned study on triple-negative breast cancer lines, silencing of the cGAS-STING-IL6-STAT3 axis by tocilizumab, a monoclonal antibody inhibiting the IL6-receptor, selectively reduced proliferation and viability of cells carrying high chromosomal instability. No significant effects were instead noted in those lines without in vitro induced chromosomal instability nor in normal epithelial breast cells [39]. Considering that increased IL6 rates have been associated with a severe prognosis in renal cell carcinoma patients [33], these results open new insights about the employment of tocilizumab or other related molecules for improving the outcome of such patients, potentially enhancing the effect of the other currently available immunotherapies. In this scenario, immunohistochemical expression of STING could be adopted as a predictive efficacy biomarker for identifying which patients affected by metastatic or morphologically aggressive tumors may benefit from immunotherapy.

In conclusion, in our study, we have demonstrated a significant association between immunohistochemical expression of STING and high-grade (G3–G4) metastatic clear cell renal



cell carcinomas, in contrast to organ-confined low-grade (G1–G2) lesions which have less frequently expressed this marker. Along with pTNM stage and the presence of coagulative granular necrosis, STING expression reached a statistically independent significance ( $p = 0.036$ ) in multivariable analysis among prognostic factors. Despite further studies being warranted for investigating its specific function in clear cell renal cell carcinomas, our data suggest a prognostic role for this marker. Moreover, experimental observations of an immunoregulative effect of the activation of the STING by aggressive tumors advocate for the potential therapeutic use of modulators of the pathway of this molecule as well, especially along with immune-checkpoints modulators.

**Supplementary Information** The online version contains supplementary material available at <https://doi.org/10.1007/s00428-023-03549-y>.

**Author contributions** Conceptualization: A. C. and G. M.; methodology: S. M., A. C., and S. P.; formal analysis and investigation: S. M. A. C., and G. B.; statistical analysis: G. B.; writing — original draft preparation: S. M. and A. C.; writing — review and editing: M. R., M. B., L. M., L. S., S. G., A. P., C. P., A. P., and A. A.; supervision: A. C. and G. M.

**Funding** Open access funding provided by Università degli Studi di Verona within the CRUI-CARE Agreement.

**Data availability** All data generated or analyzed during this study are included in this published article (and its supplementary information files).

## Declarations

**Ethical approval** All procedures involving human participants received institutional review board approval and were in accordance with the ethical standards of the institutional and/or national research committee and with the declaration of Helsinki.

**Informed consent** All patients gave their written informed consent to diagnostic procedures and treatment according to institutional rules for everyday clinical practice and experimental evaluations on archival tissue.

**Conflict of interest** The authors declare no competing interests.

**Open Access** This article is licensed under a Creative Commons Attribution 4.0 International License, which permits use, sharing, adaptation, distribution and reproduction in any medium or format, as long as you give appropriate credit to the original author(s) and the source, provide a link to the Creative Commons licence, and indicate if changes were made. The images or other third party material in this article are included in the article's Creative Commons licence, unless indicated otherwise in a credit line to the material. If material is not included in the article's Creative Commons licence and your intended use is not permitted by statutory regulation or exceeds the permitted use, you will need to obtain permission directly from the copyright holder. To view a copy of this licence, visit <http://creativecommons.org/licenses/by/4.0/>.

## References

- Motwani M, Pesiridis S, Fitzgerald KA (2019) DNA sensing by the cGAS-STING pathway in health and disease. *Nature reviews Genetics* 20:657–674. <https://doi.org/10.1038/s41576-019-0151-1>
- Cai X, Chiu Y-H, Chen ZJ (2014) The cGAS-cGAMP-STING pathway of cytosolic DNA sensing and signaling. *Molecular cell* 54:289–296. <https://doi.org/10.1016/j.molcel.2014.03.040>
- Ishikawa H, Ma Z, Barber GN (2009) STING regulates intracellular DNA-mediated, type I interferon-dependent innate immunity. *Nature* 461:788–792. <https://doi.org/10.1038/nature08476>
- Ishikawa H, Barber GN (2008) STING is an endoplasmic reticulum adaptor that facilitates innate immune signalling. *Nature* 455:674–678. <https://doi.org/10.1038/nature07317>
- Archer KA, Durack J, Portnoy DA (2014) STING-dependent type I IFN production inhibits cell-mediated immunity to *Listeria monocytogenes*. *PLoS pathogens* 10:e1003861. <https://doi.org/10.1371/journal.ppat.1003861>
- Lam E, Stein S, Falck-Pedersen E (2014) Adenovirus detection by the cGAS/STING/TBK1 DNA sensing cascade. *Virology journal* 88:974–981. <https://doi.org/10.1128/JVI.02702-13>
- Maringer K, Fernandez-Sesma A (2014) Message in a bottle: lessons learned from antagonism of STING signalling during RNA virus infection. *Cytokine and Growth Factor Reviews* 25:669–679. <https://doi.org/10.1016/j.cytogfr.2014.08.004>
- Janko C, Schorn C, Grossmayer GE, Frey B, Herrmann M, Gaip US, Munoz LE (2008) Inflammatory clearance of apoptotic remnants in systemic lupus erythematosus (SLE). *Autoimmunity reviews* 8:9–12. <https://doi.org/10.1016/j.autrev.2008.07.015>
- Hootman JM, Helmick CG, Barbour KE, Theis KA, Boring MA (2016) Updated projected prevalence of self-reported doctor-diagnosed arthritis and arthritis-attributable activity limitation among US adults, 2015–2040. *Arthritis and Rheumatology (Hoboken, N.J.)* 68:1582–1587. <https://doi.org/10.1002/art.39692>
- Wei B, Xu L, Guo W, Wang Y, Wu J, Li X, Cai X, Hu J, Wang M, Xu Q, Liu W, Gu Y (2021) SHP2-mediated inhibition of DNA repair contributes to cGAS-STING activation and chemotherapeutic sensitivity in colon cancer. *Cancer research* 81(12):3215–3228. <https://doi.org/10.1158/0008-5472.CAN-20-3738>
- Kitajima S, Ivanova E, Guo S, Yoshida R, Campisi M, Sundararaman SK, Tange S, Mitsuishi Y, Thai TC, Masuda S, Piel BP, Sholl LM, Kirschmeier PT, Paweletz CP, Watanabe H, Yajima M, Barbie DA (2019) Suppression of STING associated with LKB1 loss in KRAS-driven lung cancer. *Cancer Discovery* 9:34–45. <https://doi.org/10.1158/2159-8290.CD-18-0689>
- Gilmore E, McCabe N, Kennedy RD, Parkes EE (2019) DNA repair deficiency in breast cancer: opportunities for immunotherapy. *Journal of oncology* 2019:4325105. <https://doi.org/10.1155/2019/4325105>
- Caliò A, Brunelli M, Gobbo S, Pedron S, Segala D, Argani P, Martignoni G (2021) Stimulator of interferon genes (STING) immunohistochemical expression in the spectrum of perivascular epithelioid cell (PEC) lesions of the kidney. *Pathology* 53(5):579–585. <https://doi.org/10.1016/j.pathol.2020.09.025>
- Msaouel P, Malouf GG, Su X, Yao H, Tripathi DN, Soeung M, Gao J, Rao P, Coarfa C, Creighton CJ, Bertocchio J-P, Kunimallaiyaan S, Multani AS, Blando J, He R, Shapiro DD, Perelli L, Srinivasan S, Carbone F et al (2020) Comprehensive molecular characterization identifies distinct genomic and immune hallmarks of renal medullary carcinoma. *Cancer Cell* 37:720–734. e13. <https://doi.org/10.1016/j.ccell.2020.04.002>

15. Binnewies M, Roberts EW, Kersten K, Chan V, Fearon DF, Merad M, Coussens LM, Gaborovich DI, Ostrand-Rosenberg S, Hedrick CC, Vonderheide RH, Pittet MJ, Jain RK, Zou W, Howcroft TK, Woodhouse EC, Weinberg RA, Krummel MF (2018) Understanding the tumor immune microenvironment (TIME) for effective therapy. *Nature medicine* 24:541–550. <https://doi.org/10.1038/s41591-018-0014-x>
16. Takahara T, Murase Y, Tsuzuki T (2021) Urothelial carcinoma: variant histology, molecular subtyping, and immunophenotyping significant for treatment outcomes. *Pathology* 53:56–66. <https://doi.org/10.1016/j.pathol.2020.09.004>
17. Delahunt B, McKenney JK, Lohse CM, Leibovich BC, Thompson RH, Boorjian SA, Chevillet JC (2013) A novel grading system for clear cell renal cell carcinoma incorporating tumor necrosis. *American Journal of Surgical Pathology* 37:311–322. <https://doi.org/10.1097/PAS.0b013e318270f71c>
18. WHO Classification of Tumours (2022) Urinary and male genital tumours, WHO Classification of Tumours Editorial Board, 5th edn. IARC press, Lyon
19. Delahunt B, Chevillet JC, Martignoni G, Humphrey PA, Magi-Galluzzi C, McKenney J, Egevad L, Algaba F, Moch H, Grignon DJ, Montironi R, Srigley JR (2013) The International Society of Urological Pathology (ISUP) grading system for renal cell carcinoma and other prognostic parameters. *American Journal of Surgical Pathology* 37:1490–1504. <https://doi.org/10.1097/PAS.0b013e318299f0fb>
20. Samaratunga H, Delahunt B, Srigley JR, Berney DM, Cheng L, Evans A, Furusato B, Leite KRM, MacLennan GT, Martignoni G, Moch H, Pan C-C, Paner G, Ro J, Thunders M, Tsuzuki T, Wheeler T, van der Kwast T, Varma M et al (2020) Granular necrosis: a distinctive form of cell death in malignant tumours. *Pathology* 52:507–514. <https://doi.org/10.1016/j.pathol.2020.06.002>
21. Galfano A, Novara G, Iafrate M, Cavalleri S, Martignoni G, Gardiman M, D'Elia C, Patard JJ, Artibani W, Ficarra V (2008) Mathematical models for prognostic prediction in patients with renal cell carcinoma. *Urologia internationalis* 80:113–123. <https://doi.org/10.1159/000112599>
22. Lane BR, Kattan MW (2008) Prognostic models and algorithms in renal cell carcinoma. *Urologic Clinics of North America* 35:613–625. <https://doi.org/10.1016/j.ucl.2008.07.003>
23. Wang X, Xu H, Guo M, Shen Y, Li P, Wang Z, Zhan M (2021) The use of an oxidative stress scoring system in prognostic prediction for kidney renal clear cell carcinoma. *Cancer communications (London, England)* 41:354–357. <https://doi.org/10.1002/cac2.12152>
24. Massari F, Ciccarese C, Porcaro AB, Ferrero S, Gazzano G, Artibani W, Modena A, Bria E, Sava T, Calì A, Novara G, Ficarra V, Chilosi M, Martignoni G, Bosari S, Cheng L, Tortora G, Brunelli M (2014) Quantitative score modulation of HSP90 and HSP27 in clear cell renal cell carcinoma. *Pathology* 46:523–526. <https://doi.org/10.1097/PAT.0000000000000150>
25. Freund A, Laberge R-M, Demaria M, Campisi J (2012) Lamin B1 loss is a senescence-associated biomarker. *Molecular Biology of the Cell* 23:2066–2075. <https://doi.org/10.1091/mbc.E11-10-0884>
26. Glück S, Guey B, Gulen MF, Wolter K, Kang T-W, Schmacke NA, Bridgeman A, Rehwinkel J, Zender L, Ablasser A (2017) Innate immune sensing of cytosolic chromatin fragments through cGAS promotes senescence. *Nature cell biology* 19:1061–1070. <https://doi.org/10.1038/ncb3586>
27. Corrales L, Glickman LH, McWhirter SM, Kanne DB, Sivick KE, Katibah GE, Woo S-R, Lemmens E, Banda T, Leong JJ, Metchette K, Dubensky TWJ, Gajewski TF (2015) Direct activation of STING in the tumor microenvironment leads to potent and systemic tumor regression and immunity. *Cell reports* 11:1018–1030. <https://doi.org/10.1016/j.celrep.2015.04.031>
28. Larkin B, Ilyukha V, Sorokin M, Buzdin A, Vannier E, Poltorak A (2017) Cutting edge: activation of STING in T cells induces type I IFN responses and cell death. *Journal of Immunology* 199:397–402. <https://doi.org/10.4049/jimmunol.1601999>
29. Dou Z, Ghosh K, Vizioli MG, Zhu J, Sen P, Wangenstein KJ, Simithy J, Lan Y, Lin Y, Zhou Z, Capell BC, Xu C, Xu M, Kieckhafer JE, Jiang T, Shoshkes-Carmel M, Al Tanim KMA, Barber GN, Seykora JT et al (2017) Cytoplasmic chromatin triggers inflammation in senescence and cancer. *Nature* 550:402–406. <https://doi.org/10.1038/nature24050>
30. Yang H, Wang H, Ren J, Chen Q, Chen ZJ (2017) cGAS is essential for cellular senescence. *Proceedings of the National Academy of Sciences* 114:E4612–E4620. <https://doi.org/10.1073/pnas.1705499114>
31. Bakhom SF, Landau DA (2017) Chromosomal instability as a driver of tumor heterogeneity and evolution. *Cold Spring Harbor perspectives in medicine* 7(6):a029611. <https://doi.org/10.1101/cshperspect.a029611>
32. Yan H, Lu W, Wang F (2023) The cGAS-STING pathway: a therapeutic target in chromosomally unstable cancers., *Signal Transduct. Targeted Therapy* 8:45. <https://doi.org/10.1038/s41392-023-01328-4>
33. Wang Y, Zhang Y (2020) Prognostic role of interleukin-6 in renal cell carcinoma: a meta-analysis. *Clinical and Translational Oncology* 22:835–843. <https://doi.org/10.1007/s12094-019-02192-x>
34. Davis D, Tretiakova MS, Kizzar C, Woltjer R, Krajchich V, Tykodi SS, Lanciault C, Andeen NK (2020) Abundant CD8+ tumor infiltrating lymphocytes and beta-2-microglobulin are associated with better outcome and response to interleukin-2 therapy in advanced stage clear cell renal cell carcinoma. *Annals of diagnostic pathology* 47:151537. <https://doi.org/10.1016/j.anndiagpath.2020.151537>
35. Motzer R, Alekseev B, Rha S-Y, Porta C, Eto M, Powles T, Grünwald V, Hutson TE, Kopyltsov E, Méndez-Vidal MJ, Kozlov V, Alyasova A, Hong S-H, Kapoor A, Alonso Gordoia T, Merchan JR, Winquist E, Maroto P, Goh JC et al (2021) Lenvatinib plus pembrolizumab or everolimus for advanced renal cell carcinoma., *N. The New England Journal of Medicine* 384:1289–1300. <https://doi.org/10.1056/NEJMoa2035716>
36. Motzer RJ, Robbins PB, Powles T, Albiges L, Haanen JB, Larkin J, Mu XJ, Ching KA, Uemura M, Pal SK, Alekseev B, Gravis G, Campbell MT, Penkov K, Lee JL, Hariharan S, Wang X, Zhang W, Wang J et al (2020) Avelumab plus axitinib versus sunitinib in advanced renal cell carcinoma: biomarker analysis of the phase 3 JAVELIN Renal 101 trial. *Nature medicine* 26:1733–1741. <https://doi.org/10.1038/s41591-020-1044-8>
37. Powles T, Plimack ER, Soulières D, Waddell T, Stus V, Gafanov R, Nosov D, Pouliot F, Melichar B, Vynnychenko I, Azevedo SJ, Borchiellini D, McDermott RS, Bedke J, Tamada S, Yin L, Chen M, Molife LR, Atkins MB, Rini BI (2020) Pembrolizumab plus axitinib versus sunitinib monotherapy as first-line treatment of advanced renal cell carcinoma (KEYNOTE-426): extended follow-up from a randomised, open-label, phase 3 trial. *The Lancet Oncology* 21:1563–1573. [https://doi.org/10.1016/S1470-2045\(20\)30436-8](https://doi.org/10.1016/S1470-2045(20)30436-8)
38. Bakhom SF, Ngo B, Laughney AM, Cavallo J-A, Murphy CJ, Ly P, Shah P, Sriram RK, Watkins TBK, Taunk NK, Duran M, Pauli C, Shaw C, Chadalavada K, Rajasekhar VK, Genovese G, Venkatesan S, Birkbak NJ, McGranahan N et al (2018) Chromosomal instability drives metastasis through a cytosolic DNA response. *Nature* 553:467–472. <https://doi.org/10.1038/nature25432>
39. Hong C, Schubert M, Tijhuis AE, Requesens M, Roorda M, van den Brink A, Ruiz LA, Bakker PL, van der Sluis T, Pieters W, Chen M, Wardenaar R, van der Vegt B, Spierings DCJ, de Bruyn M, van Vugt MATM, Fojer F (2022) cGAS-STING drives the IL-6-dependent survival of chromosomally unstable cancers. *Nature* 607:366–373. <https://doi.org/10.1038/s41586-022-04847-2>

**Publisher's note** Springer Nature remains neutral with regard to jurisdictional claims in published maps and institutional affiliations.